CDF note 9824

A Measurement of $t\bar{t}$ Spin Correlations Coefficient in 2.8 fb^{-1} Dilepton Candidates

The CDF Collaboration
URL http://www-cdf.fnal.gov
(Dated: June 24, 2009)

One of the most remarkable properties of the top quark is its extremely short lifetime, which allows us to observe the top quark spin at its production. That means a spin correlation at $t\bar{t}$ production is possible to be observed. In this note, we report on a measurement of the correlation coefficient between t spin and $\bar{t}$ spin in the off-diagonal basis at $t\bar{t}$ production/decay in $p\bar{p}$ collisions at $\sqrt{s} = 1.96$ TeV using dilepton candidates observed in 2.8 fb^{-1} beam data.

We determine 68% confidence interval for the correlation coefficient κ as

$$-0.455 < \kappa < 0.865 \text{ (68\%C.L.)}$$

or

$$\kappa = 0.320^{+0.545}_{-0.775}$$

on the assumption of $M_{\rm top} = 175$ GeV/c^2.

Preliminary Results as of June 2009

I. INTRODUCTION

This note describes a measurement of the correlation coefficient between t spin and $\bar{t}$ spin in the off-diagonal basis [1] at $t\bar{t}$ production and/or decay in $p\bar{p}$ collisions at $\sqrt{s} = 1.96$ TeV using dilepton candidates observed in 2.8 fb^{-1} beam data with the CDF detector at the Fermilab Tevatron.

The standard model predicts the top quark retain its original polarization at the production until decay [2], and due to the decay via parity violating weak interaction, the information of the parent top polarization is transfered to decay products. This means we can directly observe the polarization of top quark spin when it's produced, and of powerful use to a probe of $t\bar{t}$ production mechanism. The spin-spin correlation at $t\bar{t}$ production is expected to be observed through correlations between flight directions of decay products.

In this analysis, we measure κ, the correlation coefficient at the $t\bar{t}$ decay in the dilepton channel, where $t\bar{t}$ is supposed to decay with the following differential cross section and decay rate:

$$\frac{1}{\sigma}\frac{d^2\sigma}{d\cos\theta_+ d\cos\theta_-} = \frac{1+\kappa\cos\theta_+\cos\theta_-}{4} \ , \tag{1}$$

where $\theta_+(\theta_-)$ denotes the angle of flight direction of $\ell^+(\ell^-)$ with respect to the quantization axis of the top (anti-top) quark.

The spin correlation depends on the quantization basis for top and anti-top spin. We select the off-diagonal basis where the correlation is expected maximum for $t\bar{t}$ pair production through $q\bar{q}$ annihilation. In this basis, the standard model predicts κ is close to 1. Including a contribution from $t\bar{t}$ pair production through gg fusion, κ is predicted to about 0.8 [3].

If we observe non-zero correlation coefficient κ in $t\bar{t}$ production and/or decay, that consequently indicates the direct evidence that top and anti-top are produced with their spins correlated and decay as bare quarks before losing their spin polarizations.

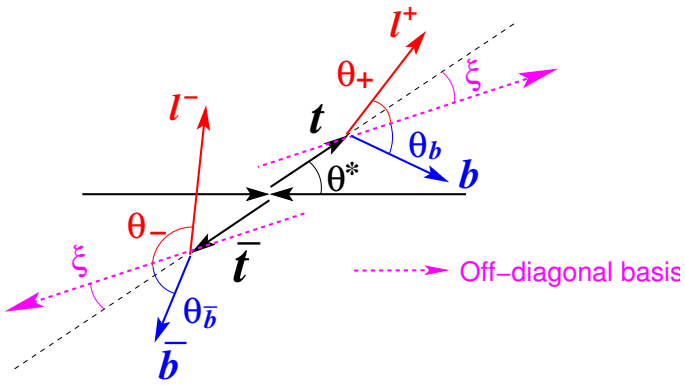

FIG. 1: Definitions of θ^*, off-diagonal basis, θ_+, θ_-, θ_b, and $\theta_{\bar{b}}$. θ^* is defined as the angle of top flight direction with respect to the proton direction in $t\bar{t}$ center of mass frame. The off-diagonal basis is defined as axes with an angle ξ toward clockwise direction from top and anti-top flight direction, respectively. θ_+, θ_-, θ_b, and $\theta_{\bar{b}}$ are angles of ℓ^+, ℓ^-, b, and $\bar{b}$ flight direction with respect to each quantization axis for top and anti-top in top and anti-top rest frames, respectively.

The off-diagonal basis is defined by an angle ξ in Fig. 1. The angle ξ is

$$\tan\xi = \sqrt{1-\beta^2}\tan\theta^* \ , \tag{2}$$

where β is top quark velocity in $t\bar{t}$ center of mass frame. Fig. 1 also shows the definition of θ_+, θ_-, θ_b, and $\theta_{\bar{b}}$, and we use the distributions of ($\cos\theta_+$, $\cos\theta_-$) and ($\cos\theta_b$, $\cos\theta_{\bar{b}}$) to extract the spin correlation.

In this analysis, we used 195 $t\bar{t}$ candidates in dilepton channel observed in CDFII detector. The detail of the detector is described in [4].

II. DATA SAMPLE AND EVENT SELECTION

This analysis is based on an integrated luminosity of 2.8 fb^{-1} collected with the CDFII detector between March 2002 and April 2008. The data are collected with an inclusive lepton trigger that requires an electron or muon with

$E_T > 18$ GeV ($p_T > 18$ GeV/c for the muon). From this inclusive lepton dataset we select events offline with two high p_T charged leptons from W decays, large missing E_T ($\not\!\!E_T$) due to two missing neutrinos, and two jets originating from b-quarks. The detailed selection criteria are described in [5]. We here briefly summarize the selection criteria (We call DIL selection hereafter):

- Two electrons or muons with $E_T > 20$ GeV for electrons and $p_T > 20$ GeV/c for muons. At least one of them is required to be in the central region and at least one of them must be isolated.
- If the event has a lepton originates from γ conversion or a track of cosmic particle, the event is rejected.
- $\not\!\!E_T > 25$ GeV.
- $\not\!\!E_T > 50$ GeV or the angle between $\not\!\!E_T$ and any lepton or jet direction projected on the azimuthal plane in the event is required to be greater than 20°.
- Two or more jets with $E_T > 15$ GeV after a energy correction and $|\eta| < 2.5$.
- Z-event veto: If the event has same flavor lepton pair with its invariant mass in $76 < M_{\ell\ell} < 106$ GeV/c^2, the missing E_T significance $\not\!\!E_T/\sqrt{\sum E_T} > 4$ is required.
- Scaler sum of E_T's of leptons, jets, and missing energy: $H_T > 200$ GeV.
- The lepton pair has to have opposite charge.

The dominant background processes remained after the DIL selection are diboson production ($WW/WZ/ZZ$), Drell-Yan ($q\bar{q} \to Z/\gamma^* \to ee, \mu\mu, \tau\tau$), and W+jets production where one jet is misidentified as a charged lepton. Considerably small contribution comes from $W\gamma$ production.

The number of $t\bar{t}$ signal and backgrounds expected with the data corresponds to 2.8 fb^{-1} are estimated using Monte Carlo simulation as well as data in control regions, and summarized in Table I.

TABLE I: The table of expected number of events in data correspond to 2.8 fb^{-1} with the observed number of events.

Process	Number of expected events
WW	9.46 ± 1.63
WZ	2.21 ± 0.36
ZZ	1.51 ± 1.19
Drell-Yan($Z \to ee, \mu\mu$)	20.68 ± 3.03
$Z \to \tau\tau$	7.30 ± 1.41
Fakes	34.15 ± 9.74
$W\gamma$	0.23 ± 0.25
Total background	75.54 ± 11.72
$t\bar{t}(\sigma = 6.7$ pb)	130.30 ± 9.92
Total SM expectation	205.84 ± 18.77
Data (2.8 fb^{-1})	195

III. SIGNAL AND BACKGROUND TEMPLATES

We use the expected distributions of ($\cos\theta_+$, $\cos\theta_-$) and ($\cos\theta_b$, $\cos\theta_{\bar{b}}$) of the $t\bar{t}$ signal and background as signal and background templates to calculate a likelihood of observed reconstructed distributions as a function of assumed κ. Then we extract a measured κ that gives the maximum likelihood. For the $t\bar{t}$ signal, therefore, the templates should be as a function of κ.

A. Full kinematical reconstruction in dilepton channel

In a dilepton event, we have six unknown variables come from two neutrino momenta ($\vec{p}_\nu$, $\vec{p}_{\bar{\nu}}$). If we suppose momenta of ℓ^+, ℓ^-, b and $\bar{b}$ are observables, we have the following six constraints:

$$\begin{aligned} M^2_{\ell^+\nu} = M^2_{\ell^-\bar{\nu}} &= M^2_W \\ M^2_{\ell^+\nu b} = M^2_{\ell^-\bar{\nu}\bar{b}} &= M^2_t \\ \vec{p}_\nu + \vec{p}_{\bar{\nu}} &= \vec{\not{E}}_T. \end{aligned} \tag{3}$$

Since the system above has same number of unknown variables and constraints, we typically have two or four possible solutions of ($\vec{p}_\nu$, $\vec{p}_{\bar{\nu}}$).

In an actual event, we suppose momenta of ℓ^+, ℓ^-, jet1, jet2, and $\vec{\not{E}}_T$ are observables, and taking resolutions of jet energies and $\not{E}_T$ into account, we define the following likelihood as a function of assumed $\vec{p}_\nu$, $\vec{p}_{\bar{\nu}}$, $E_b^{\rm guess}$, and $E_{\bar{b}}^{\rm guess}$:

$$\begin{aligned} \mathcal{L}\left(\vec{p}_\nu, \vec{p}_{\bar{\nu}}, E_b^{\rm guess}, E_{\bar{b}}^{\rm guess}\right) = P\left(p_z^{t\bar{t}}\right) P\left(p_T^{t\bar{t}}\right) P\left(M_{t\bar{t}}\right) \times \\ \frac{1}{\sigma_b} \exp\left[-\frac{1}{2}\left\{\frac{E_b^{\rm meas} - E_b^{\rm guess}}{\sigma_b}\right\}^2\right] \times \frac{1}{\sigma_{\bar{b}}} \exp\left[-\frac{1}{2}\left\{\frac{E_{\bar{b}}^{\rm meas} - E_{\bar{b}}^{\rm guess}}{\sigma_{\bar{b}}}\right\}^2\right] \times \\ \frac{1}{\sigma_x^{\rm MET}} \exp\left[-\frac{1}{2}\left\{\frac{\not{E}_x^{\rm meas} - \not{E}_x^{\rm guess}}{\sigma_x^{\rm MET}}\right\}^2\right] \times \frac{1}{\sigma_y^{\rm MET}} \exp\left[-\frac{1}{2}\left\{\frac{\not{E}_y^{\rm meas} - \not{E}_y^{\rm guess}}{\sigma_y^{\rm MET}}\right\}^2\right], \end{aligned} \tag{4}$$

where $P\left(p_z^{t\bar{t}}\right)$, $P\left(p_T^{t\bar{t}}\right)$, and $P\left(M_{t\bar{t}}\right)$ are probability density functions of each variable in a DIL candidate, which are obtained from candidates in $t\bar{t}$ Monte Carlo sample with PYTHIA [6] event generator. $E_{b,\bar{b}}^{\rm meas}$ denote the measured energy of the jets which are assigned as b- and $\bar{b}$-jets, respectively. $\not{E}_{x,y}^{\rm meas}$ are x, y components of $\vec{\not{E}}_T$. $\sigma_{b,\bar{b}}$ and $\sigma_{x,y}^{\rm MET}$ denote resolutions of measured jet energies and $\not{E}_T$. $\not{E}_{x,y}^{\rm guess}$ are x, y components of $\vec{p}_\nu + \vec{p}_{\bar{\nu}}$, respectively.

We take one representative set of ($\vec{p}_\nu$, $\vec{p}_{\bar{\nu}}$, $E_b^{\rm guess}$, $E_{\bar{b}}^{\rm guess}$) which gives maximum likelihood in each event. The likelihood is calculated in both of two cases for b-$\bar{b}$ assignments, and the assignment which gives the better likelihood is chosen as the best solution.

B. Signal template as a function of κ

We use a $t\bar{t}$ Monte Carlo sample generated by PYTHIA with $M_t = 175$ GeV/c^2. In this sample, there is no spin correlation between generated t and $\bar{t}$. We put a weight proportional to $1 + \kappa \cos\theta_+^{\rm true} \cos\theta_-^{\rm true}$ on a DIL candidate in the Monte Carlo sample, where κ is assumed spin-spin correlation coefficient in the off-diagonal basis and $\cos\theta_\pm^{\rm true}$ represent true $\cos\theta_\pm$ using the event generator information. Then, we obtain the distributions of reconstructed $(\cos\theta_+, \cos\theta_-)$ and $(\cos\theta_b, \cos\theta_{\bar{b}})$ for DIL candidates from weighed $t\bar{t}$ signal on the assumption of κ.

We use the following polynomial function to fit the distributions of reconstructed $(\cos\theta_+, \cos\theta_-)$ and $(\cos\theta_b, \cos\theta_{\bar{b}})$:

$$\begin{aligned} f(x,y) = \frac{C_0}{4}\Bigg\{ 1 \;-\; C_1 - C_3 - C_5 + 3C_1\frac{x^2+y^2}{2} \\ +\; C_2 xy + 5C_3\frac{x^4+y^4}{2} + C_4\frac{x^3y+xy^3}{2} + 9C_5x^2y^2\Bigg\}\;, \end{aligned} \tag{5}$$

where

$$\int_{-1}^{1} dx \int_{-1}^{1} dy f(x,y) = C_0\;.$$

We made the 10 by 10 bin distributions of reconstructed $(\cos\theta_+, \cos\theta_-)$ and $(\cos\theta_b, \cos\theta_{\bar{b}})$ from weighted DIL candidates in $t\bar{t}$ Monte Carlo sample on the assumption of κ ranging from -1 to 1 with 0.2 step. For each distribution we fit the resultant distribution to the function of Eqn. (5), and obtain fit parameters $C_i^\ell (i = 1, \cdots, 5)$ for the distribution of $(\cos\theta_+, \cos\theta_-)$, and $C_i^b (i = 1, \cdots, 5)$ for the distribution of $(\cos\theta_b, \cos\theta_{\bar{b}})$ as functions of κ.

Figure 2, 3 and 4 show the reconstructed distributions and their fit results in cases of $\kappa = 1$, $\kappa = 0$, and $\kappa = -1$, respectively.

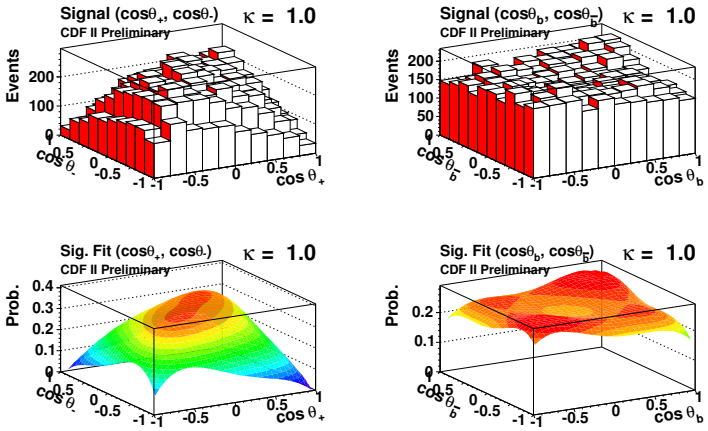

FIG. 2: The distributions of reconstructed $(\cos\theta_+, \cos\theta_-)$ (upper left) and $(\cos\theta_b, \cos\theta_{\bar{b}})$(upper right) of weighted DIL candidates in $t\bar{t}$ Monte Carlo sample on the assumption of $\kappa = 1$, and their fit results (lower left, right).

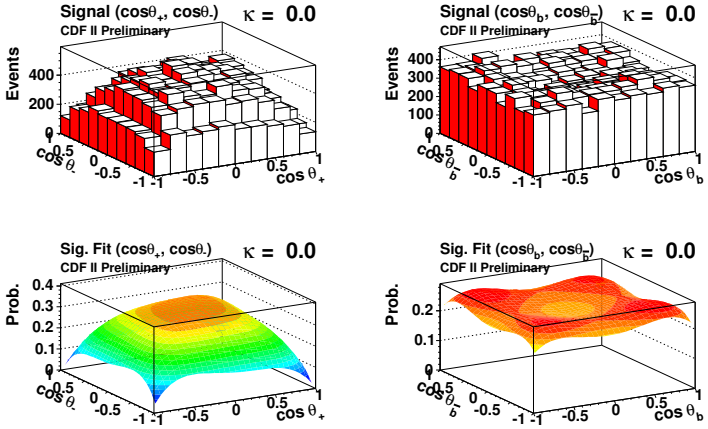

FIG. 3: The distributions and fit results on the assumption of $\kappa = 0$.

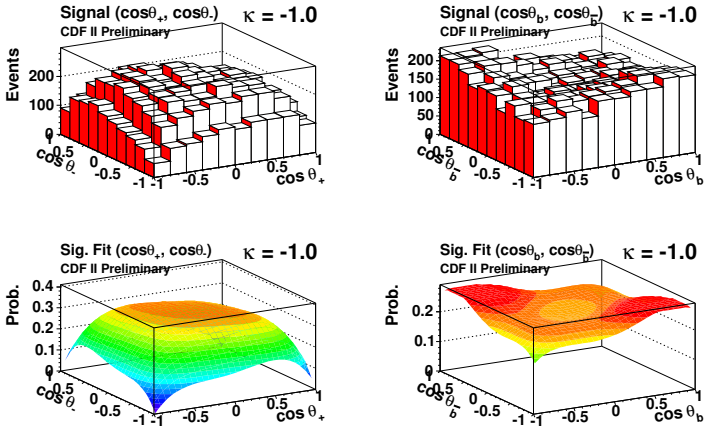

FIG. 4: The distributions and fit results on the assumption of $\kappa = -1$.

C. Background template

For background sources, we consider diboson (WW, WZ, and ZZ), Drell-Yan ($Z/\gamma^* \to ee$, $\mu\mu$ and $\tau\tau$), and fake ($W+$ jets, where W decays to e/μ and ν, and a jet is misidentified as a lepton) processes. We neglect $W\gamma$ process, since it is found to be very small contribution.

For diboson and Drell-Yan backgrounds, we estimate the background distributions using Monte Carlo basically. For the fake background, we use real data to estimate the distribution.

To estimate diboson background, We use $WW/WZ/ZZ$ Monte Carlo samples generated by PYTHIA event generator. We normalize the distributions from each sample to each expected number of events and accumulate them.

As for $Z/\gamma^* \to ee$, $\mu\mu$ and $\tau\tau$ background, we use Monte Carlo samples with exclusive processes of $Z/\gamma^* + n$ partons generated by ALPGEN [7] event generator, where Z/γ^* decays to ee, $\mu\mu$ and $\tau\tau$, respectively. We accumulate distributions from each exclusive sample with appropriate weight considering its acceptance and cross-section, then finally normalize the accumulated distribution to expected number of event of Drell-Yan background.

To obtain the distributions of fake background, we use $W+$jets sample in real beam event obtained by requiring one high p_T electron or muon, large missing E_T, and three or more jets where at least one jet can fake a lepton. We forcibly fake one of jets to an electron or muon, then set weight of the event a probability that the jet is mis-identified as the lepton. Subsequently we apply the DIL selection to the event taking the weight of each event into account, and finally normalize the distributions to expected number of events of fake background.

Finally we accumulate distributions from each component of background: $WW/WZ/ZZ$, $Z \to \tau\tau$, $Z/\gamma^* \to ee, \mu\mu$, and fake samples.

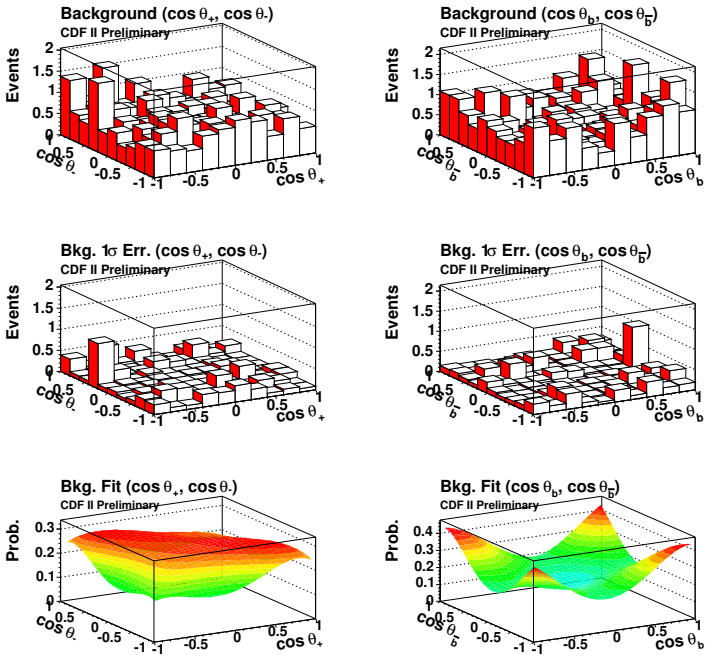

FIG. 5: The distributions of reconstructed $(\cos\theta_+, \cos\theta_-)$ (upper left) and $(\cos\theta_b, \cos\theta_{\bar{b}})$(upper right) of accumulated DIL candidates from $WW/WZ/ZZ$, $Z \to \tau\tau$, $Z/\gamma^* \to ee, \mu\mu$, and fake samples. The distributions in middle row indicate the magnitude of 1σ uncertainty of each bin of the distributions in upper row. The surfaces in the bottom row are fit results of each distribution, normalized to unit volume.

Figure 5 show the resulting distributions of reconstructed $(\cos\theta_+, \cos\theta_-)$ and $(\cos\theta_b, \cos\theta_{\bar{b}})$ for accumulated DIL candidates from all components discussed above. The distributions in middle row indicate the magnitude of 1σ uncertainty of each bin of the distributions in upper row. The surfaces in bottom row are fit results of each distribution using the same fit function form (Eqn. (5)) as the signal templates, normalized to unit volume.

The χ^2/ndf's of the fit are found to 121.661/94 for $(\cos\theta_+, \cos\theta_-)$ distribution and 103.944/94 for $(\cos\theta_b, \cos\theta_{\bar{b}})$ distribution, which are corresponding to 2.9% and 22.7% for χ^2 probabilities, respectively.

D. Cross check of reconstruction method and background modeling

We check the modeling of background and kinematical reconstruction method by comparing distributions of observed candidates in data with prediction of signal and background.

We compare one dimensional distribution of reconstructed $\cos\theta_+$ and $-\cos\theta_-$ (CP reversal of $\cos\theta_+$) in data with prediction. Also, we compare distribution of $\cos\theta_b$ and $-\cos\theta_{\bar{b}}$ in data with prediction. Note that the one dimensional distributions of $\cos\theta$ of leptons and b-jets hardly depend on κ.

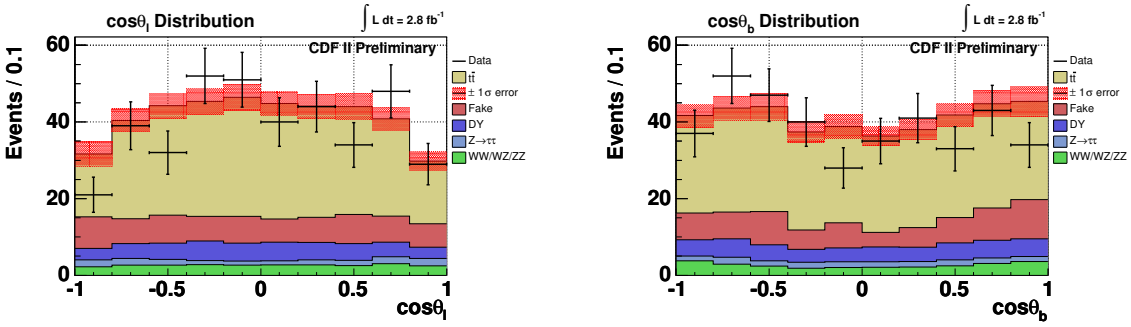

FIG. 6: The distribution of $\cos\theta_+$, $-\cos\theta_-$ (left) and $\cos\theta_b$, $-\cos\theta_{\bar{b}}$ (right). The cross indicates data and red band indicates expected number of signal and background total events with 1σ uncertainty.

Figure 6 shows the resultant distributions. The cross indicates data with statistical errors and red band indicates expected sum of signal and background events with 1σ uncertainty.

Note that since $\cos\theta$ change the sign under P reversal, an asymmetry in numbers of events between positive and negative indicates P violation. We couldn't see any obvious P violation at $t\bar{t}$ production in the off-diagonal frame.

IV. STATISTICAL AND SYSTEMATIC UNCERTAINTIES

In the previous section, signal and background templates are defined. To extract measured κ from observed distributions of reconstructed $(\cos\theta_+, \cos\theta_-)$ and $(\cos\theta_b, \cos\theta_{\bar{b}})$, we define the following likelihood as a function of assumed κ:

$$\mathcal{L}(\kappa) = \prod_i f^{\ell}(\cos\theta^i_+, \cos\theta^i_-; \kappa) f^{b}(\cos\theta^i_b, \cos\theta^i_{\bar{b}}; \kappa) \ , \tag{6}$$

where i represent index of candidates, and

$$f^{\ell,b}(x, y; \kappa) \equiv \frac{N^{\rm sig}_{\rm exp}}{N^{\rm sig}_{\rm exp} + N^{\rm bkg}_{\rm exp}} f^{\ell,b}_{\rm sig}(x, y; \kappa) + \frac{N^{\rm bkg}_{\rm exp}}{N^{\rm sig}_{\rm exp} + N^{\rm bkg}_{\rm exp}} f^{\ell,b}_{\rm bkg}(x, y) \ . \tag{7}$$

Here $N^{\rm sig}_{\rm exp}$, and $N^{\rm bkg}_{\rm exp}$ represent the expected number of events for signal and background, respectively. $f^{\ell,b}_{\rm sig}(x, y; \kappa)$, and $f^{\ell,b}_{\rm bkg}(x, y)$ represent template functions for $(\cos\theta_+, \cos\theta_-)$ and $(\cos\theta_b, \cos\theta_{\bar{b}})$ of signal and background, respectively. A measured κ, $\kappa^{\rm meas}$, is defined as a κ which gives maximum of the likelihood function.

A. Statistical uncertainty using pseudo-experiments

In this method, sensitivity to κ measurement is decided by performing pseudo-experiments.
For one pseudo-experiment, first we assume the following input values:

- true κ
- $N_{\rm obs}$: number of observed candidates
- $N^{\rm sig}_{\rm exp}$: number of expected $t\bar{t}$ signal events

- $N_{\rm exp}^{\rm bkg}$: number of expected background events

Then, we generate the following two random numbers:

- $N_{\rm obs}^{\rm sig}$: Poisson distributed number with expected value of $N_{\rm exp}^{\rm sig}$
- $N_{\rm obs}^{\rm bkg}$: Poisson distributed number with expected value of $N_{\rm exp}^{\rm bkg}$

under the condition of $N_{\rm obs}^{\rm sig} + N_{\rm obs}^{\rm bkg} = N_{\rm obs}$.

Then we pick up $N_{\rm obs}^{\rm sig}$ set of $(\cos\theta_+, \cos\theta_-)$ and $(\cos\theta_b, \cos\theta_{\bar{b}})$ randomly from $t\bar{t}$ candidate event pool of signal Monte Carlo sample generated by PYTHIA (with no spin correlation) with probability proportional to $1+\kappa\cos\theta_+^{\rm true}\cos\theta_-^{\rm true}$, and generate $N_{\rm obs}^{\rm bkg}$ random number sets of $(\cos\theta_+, \cos\theta_-)$ and $(\cos\theta_b, \cos\theta_{\bar{b}})$ which are distributed by the background templates functions.

Once $N_{\rm obs}$ pseudo events are generated, we make the likelihood function according to Eqn. (6) to obtain $\kappa^{\rm meas}$.

We perform 10K pseudo-experiments for each $\kappa^{\rm true}$ ranging from -1 to 1 with 0.1 step to obtain mean of $\kappa^{\rm meas}$ ($\langle\kappa^{\rm meas}\rangle$) and statistical uncertainty of $\kappa^{\rm meas}$ ($\sigma(\kappa^{\rm meas})$) as functions of $\kappa^{\rm true}$ on the assumption of $N_{\rm obs} = 195$, $N_{\rm exp}^{\rm sig} = 130.30$, and $N_{\rm exp}^{\rm bkg} = 75.54$. The resulting function for $\langle\kappa^{\rm meas}\rangle$ is

$$\begin{aligned} \langle\kappa^{\rm meas}\rangle &= P_0 + P_1\kappa^{\rm true}\ , \\ P_0 &= -0.0090 \pm 0.0017 \\ P_1 &= 0.9920 \pm 0.0028 \end{aligned} \tag{8}$$

and $\sigma(\kappa^{\rm meas})$ is found to about 0.79 at $\kappa^{\rm true} = 0$.

B. Systematic uncertainty

As sources of systematic uncertainty on measured κ, we consider (a) statistical fluctuation of signal Monte Carlo sample used for building the signal templates, (b) uncertainties on expected numbers of signal and background components as well as uncertainty on background templates due to statistical fluctuation of background samples, (c) uncertainty on jet energy scale (JES), (d) uncertainties on initial state radiation (ISR) and final state radiation (FSR) in Monte Carlo modeling, (e) uncertainty on parton distribution function (PDF) for initial proton and anti-proton as well as (f) fraction of $gg \to t\bar{t}$ in $t\bar{t}$ production, and (g) uncertainty on $t\bar{t}$ kinematics in the signal Monte Carlo from an effect of the next leading order calculations.

(a) Due to finite number of $t\bar{t}$ candidates in the signal Monte Carlo sample, the signal templates have statistical fluctuations. We estimate the effect on $\langle\kappa^{\rm meas}\rangle$ from $\sigma(\kappa^{\rm meas})$ obtained by performing pseudo-experiments, and found to be about 0.04 at maximum (varied as a function of κ).

(b) To estimate effects from uncertainty on expected numbers of signal and background components as well as uncertainty on background templates due to statistical fluctuation of background samples, we perform an alternative set of pseudo-experiments where we consider the fluctuations of expected number of signal events, expected numbers of each background component, and also consider statistical fluctuation of each background sample. We include the observed shift on $\langle\kappa^{\rm meas}\rangle$ and increase of $\sigma(\kappa^{\rm meas})$ in the alternative pseudo-experiments comparing with nominal pseudo-experiments into systematic uncertainty. The systematics from these effects is found to about 0.27 at maximum. This is the largest contribution to systematic uncertainty.

(c) JES uncertainty affects DIL acceptance as well as kinematical distributions. To estimate this effect, we perform pseudo-experiments where jet energy scale is shifted by $+1\sigma$ uncertainty and shifted by -1σ. Shift on $\langle\kappa^{\rm meas}\rangle$ is taken as systematics from JES uncertainty, and found to be about 0.04 at maximum.

(d) Effects from QCD initial and final state radiations are estimated using $t\bar{t}$ Monte Carlo samples specially generated with PYTHIA, in which the QCD parameters for the parton shower evolution are varied within its uncertainty. Shift on $\langle\kappa^{\rm meas}\rangle$ are taken as systematics from ISR/FSR uncertainty, and found to be about 0.06 at maximum.

(e) Systematics due to PDF uncertainties is evaluated by performing pseudo-experiments using different PDF sets for signal Monte Carlo sample, and shift on $\langle\kappa^{\rm meas}\rangle$ is taken as systematics from PDF uncertainty, and found to be about 0.20 at maximum.

(f) The nominal signal sample we use in this analysis is found to have about 6% of $t\bar{t}$ production via gluon gluon fusion process. However, this fraction is expected to be much bigger, at the level of around 15%, in case of NLO calculation [8]. The effect on $\langle\kappa^{\rm meas}\rangle$ is estimated by increasing artificially the fraction of gg fusion process, and found to be about 0.04 at maximum.

(g) An effect of NLO calculation on $t\bar{t}$ production matrix element is studied by performing pseudo-experiments using signal Monte Carlo generated with an event generator at NLO (MC@NLO [9]), and found to be about 0.14 at maximum.

C. Total uncertainty

Summing up statistical uncertainty and all possible systematic uncertainties discussed above in quadrature, we obtain total uncertainty on $\kappa^{\rm meas}$ including statistical and systematic effects. Fig. 7 shows statistical uncertainty and statistical $\oplus$ systematical uncertainties on $\kappa^{\rm meas}$ as functions of $\kappa^{\rm true}$. Systematic uncertainties toward positive and negative direction are shown separately.

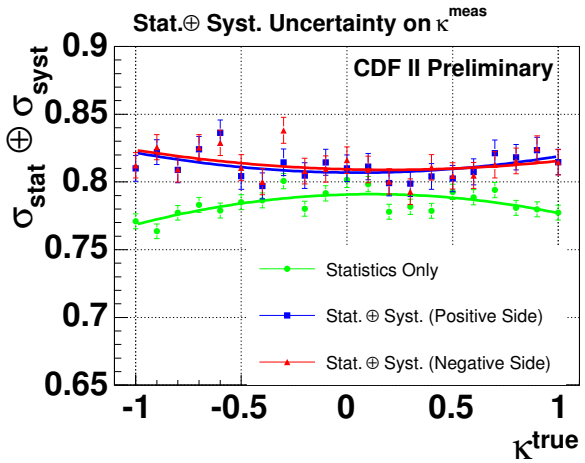

FIG. 7: Statistical uncertainty (green) and statistical $\oplus$ systematical uncertainties (blue and red) on $\kappa^{\rm meas}$ are shown separately.

Together with the function of $\langle\kappa^{\rm meas}\rangle$ (Eqn. (8)) and the total uncertainty on $\kappa^{\rm meas}$, we construct confidence belt as a function of $\kappa^{\rm true}$ according to a prescription of Feldman-Cousins's ordering principle [10] to extract a confidence interval for $\kappa^{\rm true}$ from $\kappa^{\rm meas}$.

V. RESULTS

We finally disclose the distribution of reconstructed $(\cos\theta_+, \cos\theta_-)$ and $(\cos\theta_b, \cos\theta_{\bar{b}})$ in data for integrated luminosity of 2.8 fb^{-1}, which has been kept blinded until analysis method is fixed and all studies on all possible systematics are done.

Then we calculate unbinned likelihood by Eqn. (6) to obtain $\kappa^{\rm meas}$.

Figure 8 shows the observed distributions of reconstructed $(\cos\theta_+, \cos\theta_-)$ and $(\cos\theta_b, \cos\theta_{\bar{b}})$ in data, and Fig. 9 indicates $-2\Delta\log\mathcal{L}$ as a function of κ.

From the function, we observe $\kappa^{\rm meas} = 0.309$.

Figure 10 shows the Feldman-Cousins confidence intervals constructed based on mean and uncertainty of $\kappa^{\rm meas}$ and observed result $\kappa^{\rm meas} = 0.309$. From the confidence intervals, we obtain from this the following results:

$$-0.455 < \kappa < 0.865 \text{ (68\% C.L.)} \tag{9}$$

or

$$\kappa = 0.320^{+0.545}_{-0.775} \tag{10}$$

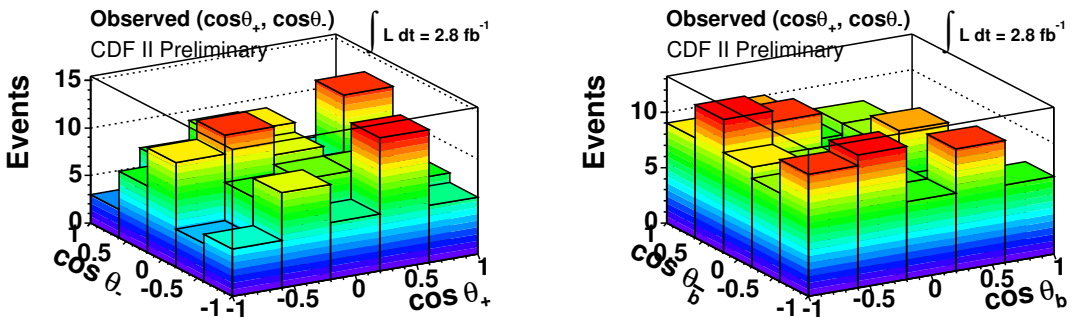

FIG. 8: Distributions of reconstructed $(\cos\theta_+, \cos\theta_-)$ (left) and $(\cos\theta_b, \cos\theta_{\bar{b}})$ (right) in 5 by 5 bins, which is observed in data for integrated luminosity of 2.8 fb^{-1}.

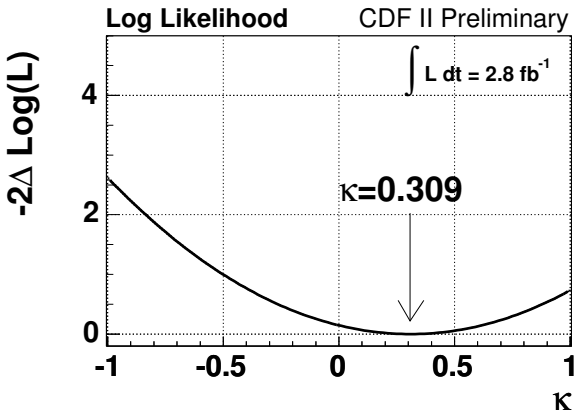

FIG. 9: $-2\Delta \log \mathcal{L}$ for the observed distributions as a function of assumed κ. The function is found to be minimum at $\kappa = 0.309$.

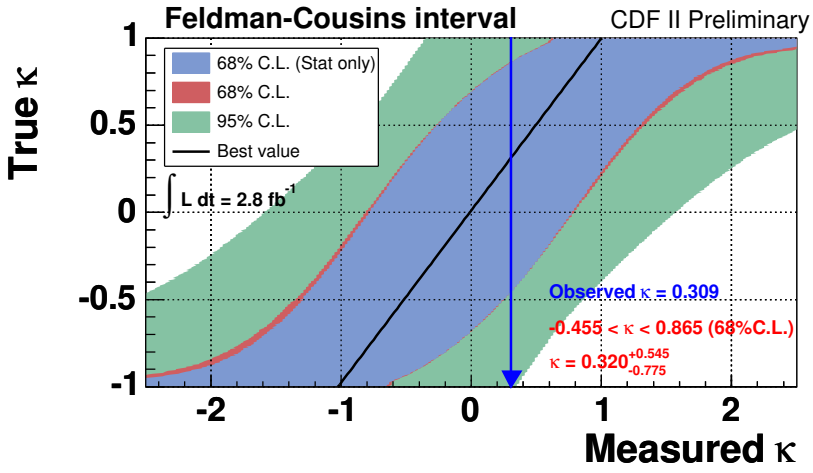

FIG. 10: Feldman-Cousins confidence intervals at 68% C.L. and 95% C.L. with observed $\kappa^{\rm meas}$. Interval at 68% C.L. on true κ corresponding to $\kappa^{\rm meas} = 0.309$ is shown.

on the assumption of $M_{\rm top} = 175$ GeV/c^2.

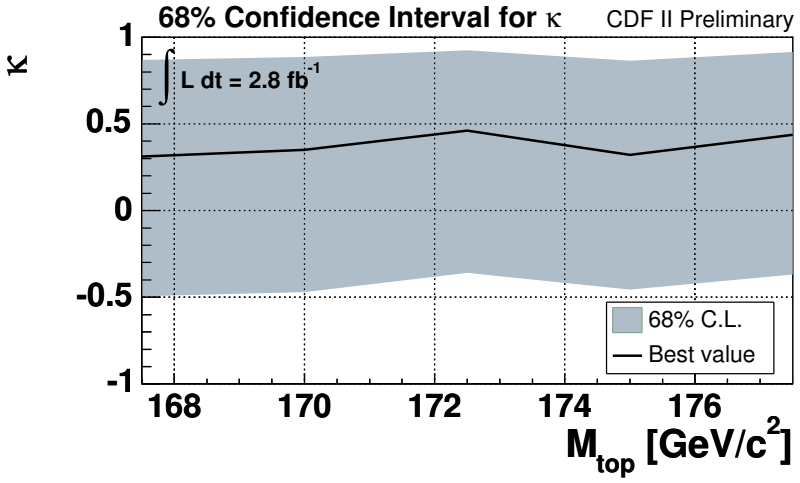

FIG. 11: 68% confidence intervals for κ as a function of assumed $M_{\rm top}$. Solid line indicates center values of κ measurement.

We also review how the result is affected on another top mass assumption. Figure 11 shows 68% confidence intervals for κ as a function of assumed $M_{\rm top}$, obtained by repeating the same analysis with different top mass assumption. Solid line indicates center values of κ measurement. We don't see any significant top mass dependence of κ measurement.

The result is consistent with the standard model prediction of $\kappa \sim 0.8$. This is the first Tevatron run II result on measurement of κ. Currently statistical uncertainty is dominated. We consequently can reduce uncertainty as to increase of integrated luminosity. At this point, we couldn't reject null correlation hypothesis, but it might be possible to reject null correlation hypothesis with more statistics in future.

Acknowledgments

We thank the Fermilab staff and the technical staffs of the participating institutions for their vital contributions. This work was supported by the U.S. Department of Energy and National Science Foundation; the Italian Istituto Nazionale di Fisica Nucleare; the Ministry of Education, Culture, Sports, Science and Technology of Japan; the Natural Sciences and Engineering Research Council of Canada; the National Science Council of the Republic of China; the Swiss National Science Foundation; the A.P. Sloan Foundation; the Bundesministerium für Bildung und Forschung, Germany; the Korean Science and Engineering Foundation and the Korean Research Foundation; the Science and Technology Facilities Council and the Royal Society, UK; the Institut National de Physique Nucleaire et Physique des Particules/CNRS; the Russian Foundation for Basic Research; the Ministerio de Ciencia e Innovación, and Programa Consolider-Ingenio 2010, Spain; the Slovak R&D Agency; and the Academy of Finland.

[1] G. Mahlon and Stephen Parke, Phys. Lett. **B 411**(1997)173
[2] A. F. Falk and M. E. Peskin, Phys. Rev. **D 49**(1994)3320; T. Stelzer and S. Willenbrock, Phys. Lett. **B 374**(1996)169
[3] W. Bernreuther *et al.*, Nucl. Phys. **B 690**(2004)81
[4] F. Abe, *et al.*, Nucl. Instum. Methods Phys. Res. **A 271**(1988)387; D. Amidei, it et al., Nucl. Instum. Methods Phys. Res. **A 350**(1994)73; F. Abe, *et al.*, Phys. Rev. **D 52**(1995)4784; P. Azzi, *et al.*, Nucl. Instrum. Methods Phys. Res. **A 360**(1995)137; The CDFII Detector Technical Design Report, Fermilab-Pub-96/390-E
[5] D. Acosta, *et al.*, Phys. Rev. Lett. **93**(2004)142001
[6] T. Sjostrand et al., High-Energy-Physics Event Generation with PYTHIA 6.1, Comput. Phys. Commun. **135**, 238 (2001).
[7] M.L. Mangano, *et al.*, a generator for hard multiparton processes in hadronic collisions, J. High Energy Phys. **0307**(2003)001
[8] N. Kidonakis *et al.*, Phys. Rev. **D 68**(2003)114014; M. Cacciari *et al.*, J. High Energy Phys. **0404**(2004)068
[9] S. Frixione and B.R. Webber, J. High Energy Phys. **0206**(2002)029; S. Frixione *et al.*, J. High Energy Phys. **0308**(2003)007
[10] G. Feldman and R. Cousins, Phys. Rev. **D 57**(1998)3873-3889